NEW STRUCTURE FOR HIGH-SENSITIVITY COAXIAL THERMAL POWER SENSOR IN THE FREQUENCY RANGE FROM DC–50 GHz

Doudou BA[1*], and Jean-Marie Lerat[1]

[1]Laboratoire National de Métrologie et d'Essais, 29 avenue Roger Hennequin, 78197 Trappes, France

Abstract. This paper presents the design and development of a new thermal microwave power sensor for a frequency range spanning from DC to 50 GHz. The purpose of this new design is to propose a high-sensitivity thermoelectric power sensor suitable for microcalorimeter application that is a primary method of microwave power calibration. The core structure of the power sensor comprises a Grounded Coplanar Waveguide (GCPW) transmission line, two load resistors, a thermopile, and output pads for DC measurements. The optimized power sensor demonstrates promising simulation performance, with a return loss better than 20 dB across the frequency range and an efficiency exceeding 80%. At 50 GHz, the sensitivity of the power sensor reaches well over 0.240 mV/mW.

1 Introduction

In various domain of sciences and engineering such as telecommunication systems and wireless applications, power sensors are used for power monitoring, control antenna gain and so on. Indeed, the development of new telecommunication protocol and microwave applications in daily life induces an increased need for reliable and traceable power measurement while in the meantime the availability of the thermistor type of sensor is becoming more and more challenging for most of National Metrology Institutes (NMIs). Therefore, research and development of new type of power sensor in the millimetre wavelengths domain is growing faster [1].

There are essentially three conventional type of power sensor such as the diode, thermistors and thermoelectric that available in the market. The general principle and method for each type of sensor is based on the detection of power by using a termination loads. Regarding the requirement of compactness, high performance in a wide frequency range, the thermoelectric are the most widely used devices to fulfil all these requirements. Extensive research has been carry out on the development of thermoelectric type of power sensor. For instance, the thermoelectric power sensor developed by Dehe et al. [2] works in the frequency range between 1 – 20 GHz and presents some limitations regarding the sensitivity of the power sensor. Wang et al. [3] and Yi et al. [4], in their work propose solutions to optimize thermoelectric power sensor performance regarding the sensitivity. By optimizing the size of the thermopile, they achieve reasonable results in return loss and sensitivity over a frequency range of 1 – 20 GHz. Recently, similar results have been achieve by Zhang et al. [5] with thermoelectric power sensor developed in GaAs process for frequency range between 1 – 30 GHz.

The main goals of this research paper are to develop and optimize a new structure of thermoelectric power sensor that shows high performances regarding the return loss, better than 20 dB, high efficiency, with high sensitivity and working in a wide frequency range. To achieve the development of a power sensor with high performances, one need full analysing of the electromagnetic response as well as the thermal response of the power sensor. Therefore, the electromagnetic-thermal co-simulation concept [6] is applied for the design and optimisation of the power sensor. The electromagnetic performance of the power sensor is analysed by using the specification of the 2.4 mm end launch connector, which operate up to 50 GHz. To obtain high sensitivity, we conduct a detail studies on the power sensor thermal properties and response when we applied microwave power.

The remaining of this paper is structured as follow. In section 2 are described the power sensors, the different components, and the design principle as well. In section 3, we provide the power sensor performances optimisation regarding the return loss, efficiency and the sensitivity.

2 Specification, design and theory of the power sensor

The overview of the different components of the power sensor is given in Fig. 1. The elements of the power sensor are à GCPW transmission line, two loads resistors as termination, a thermopile and output pads

* Corresponding author: doudou.ba@lne.fr

for DC measurements. The power sensor is fed with microwave power by using a commercial 2.4 mm end launch connector type.

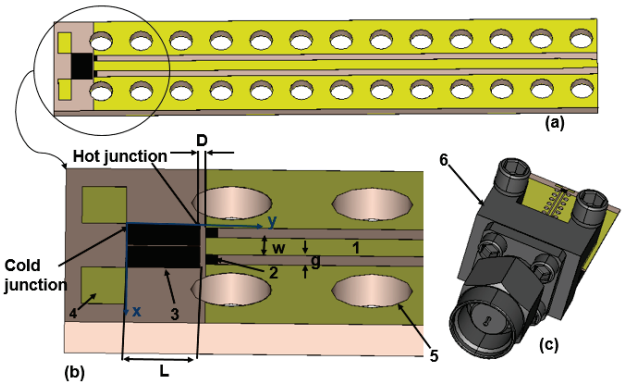

Fig. 1. (a) Internal structure of the power sensor. (b) Dimensions parameter of the power sensor. (c) 2.4 mm coaxial connector fixed to the power sensor. (1) GCPW li=transmission line, (2) load resistors, (3) thermopile, (4) output pads for Dc voltage, (5) via hole and (6) 2.4 mm coaxial connector.

The GCPW transmission line is conductor-backed coplanar waveguide (CPW). It consist of a central strip signal conductor with semi-infinite ground plane on either side, forming a ground-signal-ground structure that support quasi-TEM mode propagation. In the case of the GCPW line, an additional ground plane is located below the substrate, while a ground-signal-ground plane is deposited on top of the substrate. This additional ground plane is connected to the grounds of the upper plane by metallized vias holes [7] – [9]. The GCPW transmission line dimensions, including the width of the central strip (w) and the gap (g) between the central strip and the adjacent ground plane, were determined to achieve a characteristic impedance of 50 Ω, ensuring compatibility with the 2.4 mm end launch connector. The dimensions and positions of the vias as well as their number, were calculated and selected to prevent the appearance of a dominant rectangular waveguide mode with a cut-off frequency is given by the formula [7] below :

$$f_c = \frac{c}{2.d_{e.2e}.\sqrt{\varepsilon_r^{eff}}} \qquad (1)$$

Where c is the speed of the light, ε_r^{eff} is the effective relative dielectric constant of the substrate, $d_{e2e} = d_{c2c} - d_{via}$ is the edge-to-edge separation between two vias along the direction of the propagation, d_{c2c} is the center-to-center distance between 2 vias and d_{via} is the via diameter.

Considering the size of the power sensor, thirteen vias are placed across the direction of the propagation between the 2.4 mm end launch connector and the resistors as shown in Fig. 1. Therefore, $d_{e2e} = 0.775\ mm$ and accordingly to formula (1) above for the resonance frequency calculation is around $0.65 * f_c \cong 58\ GHz$. This is beyond the operating frequency of the power sensor designed.

For the computation, the central strip conductor, the ground planes on either side of the central strip and the additional ground at the bottom are made of thin film gold. Moreover, for the fabrication of the power sensor an additional layer of chromium is deposited on top of the substrate before thin film of gold. This additional layer is fully taken into account in the calculation and simulation.

The two parallel loads resistors are titanium sheet layer deposited at the end of the GCPW transmission line and between central strip and ground. The layer thickness is around 0.5 µm. The length (L) and the width (W) of the titanium sheet layer are optimised in order to match the 50 Ω impedance of the connectorised GCPW transmission line. Therefore the electrical resistance of each titanium sheet layer is:

$$R = \frac{R_S.L}{W} = 100\ \Omega \qquad (2)$$

The length of each titanium sheet layer is equal to the g parameter of the GCPW transmission line as shown in Fig. 1.

The couple alloy used or the thermopile is made of chrome/aluminium (Cr/Al) junctions with reasonable Seebeck coefficient. Regarding the fabrication process deposition of the Cr/Al couple alloy can be achieve by FEMTO ST (Franche-Comté Electronique Mécanique Thermique et Optiques-Sciences et Technologies) which is the manufacturing partner. The resulting output voltage (Vout) and the sensitivity (S) of the power sensor under microwave power are expressed, respectively as follow:

$$V_{out} = S_{Cr/Al} \sum_{i}^{N} \Delta T_i \qquad (3)$$

$$S = V_{out}/P_{in} \qquad (4)$$

Where $S_{Cr/Al}$ is the Seebeck coefficient of the Cr/Al alloy junctions, N is the number of thermocouples, ΔT_i correspond the temperature difference between the hot and cold junction of the thermocouples and P_{in} represent the input high frequency power.

The length of the thermopile, which refer to the distance between the hot and cold junction as shown in Fig. 1 ($L_{thermopile}$) is set at 500 µm. This value is largely sufficient for a stable ΔT_i [3]. It clearly has importance and impact on the power sensor performances, given the expression of equations (3) and (4), as the sensitivity increases when $L_{thermopile}$ is higher. However, one should consider the noise equivalent generated voltage that increase also [10] – [11], as shown by the expression of the thermal noise equivalent voltage that appears across every resistor device:

$$V_{noise} = \sqrt{4 * k_B * T_{ext} * R_e} \qquad (5)$$

Where k_B is the Boltzmann constant, T_{ext} is the external temperature and R_e is the electrical resistance of the thermopile which depends mainly to $L_{thermopile}$ parameter.

3 Power sensor electromagnetic and thermal response optimisation

3.1 Electromagnetic modelling

The modelling and the optimisation of the electromagnetic response (return loss, efficiency) of the power sensor were carried out using CST Studio Suite software. Since the GCPW transmission line is design to match 50 Ω of characteristic impedance, the power sensor matching characteristics regarding the return loss mainly depends on the positioning of the thermopile just beside the two load resistors. Therefore, we simulated the return loss performances of the power sensor with the distance between the thermopile and the two load resistors (D) in the range of 5 – 25 µm and the power sensor matching characteristic without the thermopile components is also calculated. All the power sensor components are considered as describe in section 1 and shows in Fig. 1. Fig. 2 shows the variation of the return loss across the frequency range from 1 to 50 GHz with D in range 5 – 25 µm. The results shows that the parameter D influenced the power sensor matching characteristics specifically when the frequency increase in the range 30 – 50 GHz. The return loss drop under 20 dB at 50 GHz when D = 5 µm. This degradation can be explained by the strong electromagnetic coupling effect between the thermopile and the two loads resistors when D is very small at high frequency.

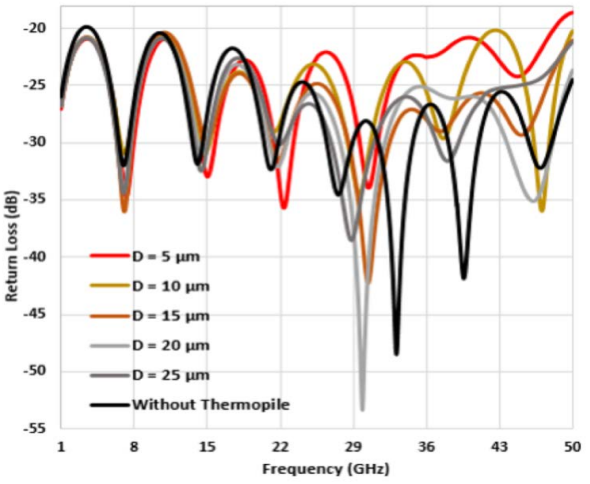

Fig. 2. Effect on changing the parameter D on the return loss of the power sensor

The power sensor effective efficiency η_{eff} as expressed in equation below correspond to the power sensor primary quantity.

$$\eta_{eff} = \frac{P_{absorbed\ by\ resistors}}{(1-\Gamma).P_{incident}} \qquad (6)$$

Where $P_{absorbed\ by\ resistors}$ is power absorbed by the resistors of the power sensor, $P_{incident}$ is power injected in the power sensor, $\Gamma = P_{reflected}/P_{incident}$ and $P_{reflected}$ is the amount of power reflected by the power sensor.

Fig. 3 shows the effective efficiency of the power sensor in the frequency range 1 – 50 GHz. As can be observed, $\eta_{effective}$ decreases when the frequency increases. When the distance D parameter in the range 15 – 20 µm, η_{eff} is higher than 80 % but it has a decreasing trend as D becomes smaller. The strong coupling effect between the thermopile and the two load resistors also affects η_{eff}, typically for D = 5 µm the effective efficiency drops below 80 % for frequency around 50 GHz.

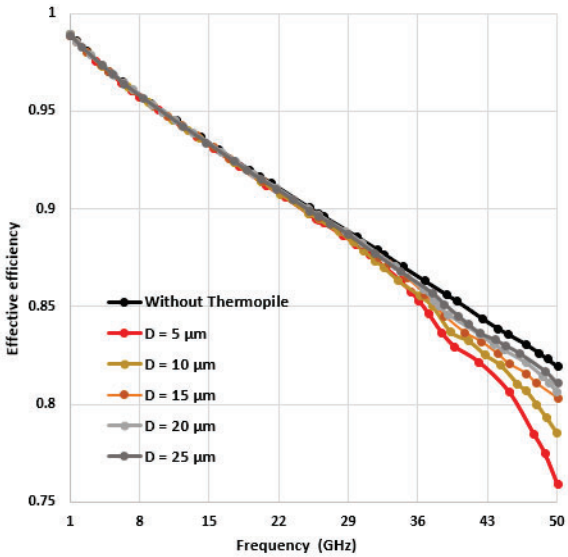

Fig. 3. Effect on changing parameter D on the effective efficiency of the power sensor

The results shows in Fig. 2 and Fig. 3 clearly highlighted the impact of the thermopile position regarding the power sensor electromagnetic response. To increase the power sensor sensitivity, one need to put the thermopile closer to the two load resistors for the temperature sensing without affecting the matching characteristics of the power sensor. Therefore, for the sensitivity analysis and calculation, the D parameter in the range of 10 – 25 µm is considered.

3.2 Thermal response and sensitivity analysis

The sensitivity calculation of a power sensor based on equation (4) depends on the thermopile sensing of the heat energy that is generated when microwave energy is absorbed and dissipated by the two load resistors. The power loss associated to the dissipated microwave power inside the power sensor depends on the electrical field distribution and the materials properties of the different components of the power sensor. The

calculation and simulation of the thermal fields can be performed by using the power loss as heat source. Therefore, a multi-physics approach is implemented by running an electromagnetic and thermal co-simulation of the power sensor response when we applied power. To carry out this co-simulation, the CST Multiphysics Solver is used. Firstly, we calculated the electromagnetic fields distributions along the materials properties to evaluate the power loss as shown in Fig. 4. The results shows power loss are mainly distributed in the area where the two load resistors are located.

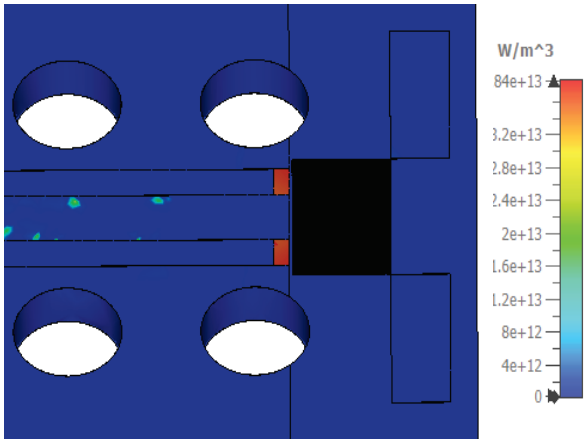

Fig. 4. Power loss density distribution of the power sensor at 50 GHz.

Table 1. Properties of materials involved in the design

Parameters	Value
Thermal conductivity (Ti)	11.3 W/(m.K)
Thermal conductivity (Au)	314 W/(m.K)
Thermal conductivity (Ni)	90.9 W/(m.K)
Thermal conductivity (Al)	90.9 W/(m.K)
Thermal conductivity (PTFE)	0.2 W/(m.K)
Thermal conductivity (Substrate)	1.5 W/(m.K)
Convection coefficient (Air)	5 W/(m.K)
Emissivity (Ti)	0.2
Emissivity (Au)	0.04
Emissivity (Substrate)	0.8
Seebeck Coefficient ($S_{Cr/Al}$)	22.5 µV/K
Ambient temperature	296.15 K
Convection coefficient (h)	5 W/(m^2.K)
Boltzman constant (k_B)	5.67* 10^{-8} W/(m^2.K^4)

The second step we performed the thermal field simulation by using the power loss results obtained in the first step as heat source. For the thermal setting, we used the parameter shown in Table 1. We consider two type of teat transfer that occurs in the power. The heat transfer by conduction between the two loads resistors, the substrate and the hot junction of the thermopile. The heat transfer by convection depends to the convective heat coefficient and the temperature difference between the surrounding air and the different components of the power sensors. Since the power sensor is design for microcalorimeter application with a maximum power level of 20 mW, we assumed the transfer type by radiation negligible and not considered for the computation and the calculation of the thermal response of the power sensor.

The temperature profile of the power sensor is shown in Fig. 5. Regarding the calculation, the parameter D is equal to 20 µm and with an applied microwave power of 10 mW through the power sensor at 50 GHz. As observed, the highest temperature value is located on the two load resistors and the nearby area. As we move away from the two load resistors layers, the temperature level decrease. This show the importance of the parameter D of the heat produce by the two load resistors.

As define in equation (4), the sensitivity of the power sensor depends on the output voltage define in equation (3). Therefore, we calculated the temperature difference between the hot and the cold junction across all the thermocouple in the thermopile as shown in Fig. 6. As expected, the temperature is maximum for hot junctions that are close to the two loads resistors. Overall, it shows a decreasing trend as we move away from the two loads resistors. It should be noted, at 50 GHz the maximum temperature difference for parameter D = 10 and D = 15 µm is very small, less than 0.1 K. This can be explain keeping in mind that the parameter η_{eff} is slightly better for D = 15 µm and as consequence the heat transfer by dissipation of the microwave power is more important.

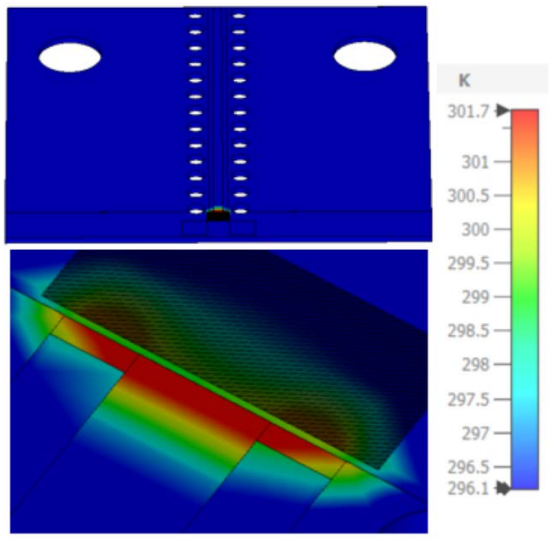

Fig. 5. (a) Thermal field distribution on the power sensor. (b) Temperature profile around the two load resistors.

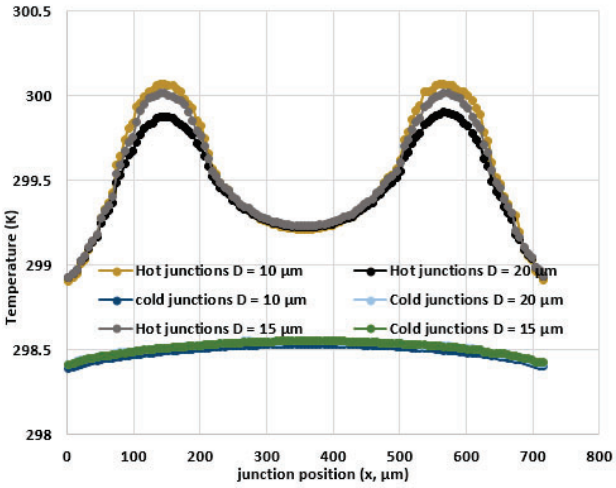

Fig. 6. Temperature distribution on the hot junctions and cold junctions of the thermopile at 50 GHz.

Fig. 7 shows the power sensor sensitivity with parameter D in the range 10 – 25 µm. The sensitivity is greater than 0.220 mV/mW across the entire frequency. At each frequency, it has a decreasing trend when parameter D increase. Regarding the performances, typically at 1 GHz, the sensitivity calculated in this paper is better when compare with similar power sensor reported in the literature.

This power sensor is design for the microcalorimeter applications with specific design goal such as reasonable return loss (up to 20 dB), efficiency higher than 80 % and high sensitivity as well. Therefore, when analysing the electromagnetic and thermal response, the power sensor with distance between the thermopile and the two load resistors of 15 µm is a reasonable compromise.

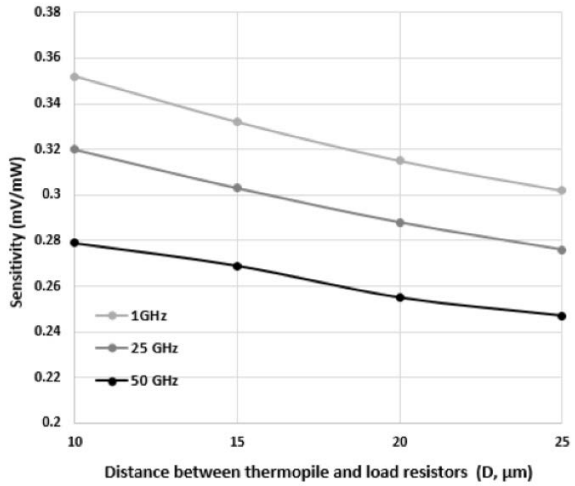

Fig. 7. Sensitivity of the power sensor vs distance between the thermopile and the two load resistors

4 Conclusion

We have reported a novel design concept of thermoelectric power for frequency range of DC – 50 GHz. The power sensor design combine a GCPW transmission line, titanium resistive load and chrome-aluminum thermopile. The optimise power sensor shows a return a loss better than 20 dB, and efficiency exceeding 80 % and high sensitivity across the entire frequency range. The sensitivity results, typically at 50 GHz, up to 0.247 mV/m was achieved which is suitable for microcalorimeter application since the applied microwave power does not exceed 20 mW.

References

1. A.S. Bush, Measurement of microwave power – A review of techniques used for measurement of high-frequency RF. IEEE Instrum. Meas. Mag. 2007, 38, 1473-1476.
2. A. Dehe, K. Fricke-Neuderth, V. Krozer, Thermoelectric power sensor for microwave applications by commercial CMOS fabrication. IEEE Electron Device Letters, 18(9), 450-452. 1997
3. D. B. Wang, X. P. Liao, T. Liu, Optimization of Indirectly-Heated Type Microwave Power Sensors Based on GaAs Micromachining. IEEE Sensors Journal, 12(5), 1349-1355. 2012
4. Z. Yi, X. Liao A 3D Model of the Thermoelectric Microwave Power Sensor by MEMS Technology. *Sensors* **2016**, *16*,921. https://doi.org/10.3390/s16060921
5. Z. Zhang, X. Liao, Zhang, Z., & Liao, X. Suspended Thermopile for Microwave Power Sensors Based on Bulk MEMS and GaAs MMIC Technology. IEEE Sensors Journal, 15(4). 2022
6. C. Mou, J. Chen, H. Peng, Electromagnetic-Thermal Co-Simulation of Planar Monopole Antenna Based on HIE-FDTD Method. MDPI-Electronics, 11(24), 4167. 2022
7. Z. Zhou, K.L. Melde, L. Development of a Broadband Coplanar Waveguide-to-Microstrip Transition with Vias. IEEE Transactions on advanced packaging, 31(4), 861-872, 2008
8. X. Hu, J. Tian, W. Tang, G. Zhang, Impact of Ground Via Placement and Size in Grounded Coplanar Waveguide Interconnects. IEEE International Workshop on Radio Frequency and Antenna Technologies, Shenzhen, China, 38-40. 2024
9. M. Grady, J.M. Kovitz, A. Iancovici, Y. Borenstein, Improved bandwidth using 3D Printed Quasi-Ideal Grounded Coplanar Waveguide Transmission Line. IEEE 22nd Annual Wireless and Microwave Technology Conference (WAMICON), Clearwater, FL, USA, 1-4. 2022.
10. O. Socher, O. Degani, Y. Nemirovskyl, Optimal consideration of CMOS compatible IR thermoelectric sensors. Sens. Act.A, vol. 71, no. 1 – 2, 107 – 115, Nov. 1998.
11. C.G. Mattsson, G. Thungstrom, K. Bertilssom, H-E Nilsson, H. Martin, Design of a Micromachined

Thermopile Infrared Sensor With a Self-Supported SiO_2/SU-8 Membrane. IEEE Sensors Journal, 8(12), 2044-2052. 2018.

12. F. Becher, Design of power sensor for measuring average power in the frequency band 110 GHz – 170 GHz, Ph.D. thesis, University of Paris-Saclay
13. S. Kodato, T. Wakabayashi, Q. Zhuang, S. Uchida, New Structure for DC-60 GHz thermal power sensor. IEEE MTT-S Int. Microw. Symp. Dig., Sanf Francisco CA, Jun. 1996, vol. 2, 871-874.